
Article:
Bright, J.A. orcid.org/0000-0002-9284-9591, Marugan-Lobon, J., Cobb, S.N. et al. (1 more author) (2016) The shapes of bird beaks are highly controlled by nondietary factors. Proceedings of the National Academy of Sciences of the United States of America, 113 (19). pp. 5352-5357. ISSN 0027-8424

https://doi.org/10.1073/pnas.1602683113

Classification: BIOLOGICAL SCIENCES; Evolution

Title: The shapes of bird beaks are highly controlled by non-dietary factors

Authors: Jen A. Bright[a,b], Jesús Marugán-Lobón[c,d], Samuel N. Cobb[e], Emily J. Rayfield[a]

Author affiliation:

[a] School of Earth Sciences, University of Bristol, Life Sciences Building, 24 Tyndall Avenue, Bristol, BS8 1TQ, United Kingdom.

[b] Department of Animal and Plant Sciences, University of Sheffield, Alfred Denny Building, Sheffield, S10 2TN, United Kingdom.

[c] Unidad de Paleontología, Dpto. Biología, Universidad Autónoma de Madrid, C/Darwin 2, Cantoblanco, Madrid 28049, Spain.

[d] Dinosaur Institute, Natural History Museum of Los Angeles County, 900 Exposition Boulevard, Los Angeles, CA 90007, USA.

[e] Department of Archaeology and Hull York Medical School, University of York, York, YO10 5DD, United Kingdom.

Corresponding authors:

Jen A. Bright. Department of Animal and Plant Sciences, University of Sheffield, Alfred Denny Building, Sheffield, S10 2TN, United Kingdom. +44(0)114 222 0079. jen.bright@gmail.com.

Keywords: Geometric Morphometrics; Integration; Allometry; Birds; Modularity

Abstract:

Bird beaks are textbook examples of ecological adaptation to diet, but their shapes are also controlled by genetic and developmental histories. To test the effects of these factors on the avian craniofacial skeleton, we conducted morphometric analyses on raptors, a polyphyletic group at the base of the landbird radiation. Despite common perception, we find that the beak is not an independently targeted module for selection. Instead, the beak and skull are highly integrated structures strongly regulated by size, with axes of shape change linked to the actions of recently identified regulatory genes. Together, size and integration account for almost 80% of the shape variation seen between different species to the exclusion of morphological dietary adaptation. Instead, birds of prey use size as a mechanism to modify their feeding ecology. The extent to which shape variation is confined to a few major axes may provide an advantage in that it facilitates rapid morphological evolution via changes in body size, but may also make raptors especially vulnerable when selection pressures act against these axes. The phylogenetic position of raptors suggests that this constraint is prevalent in all landbirds, and that breaking the developmental correspondence between beak and braincase may be the key novelty in classic passerine adaptive radiations.

Significance Statement:

We show that beak and skull shapes in birds of prey ("raptors") are strongly coupled, and largely controlled by size. This relationship means that, rather than being able to respond independently to natural selection, beak shapes are highly constrained to evolve in a particular way. The main aspects of shape variation appear to correspond with specific genes active during development. Because raptors are not each other's closest relatives, similar shape constraints may therefore have been present in the ancestors of all modern songbirds including Darwin's finches, the classic example of explosive evolution in birds. If this hypothesis is true, then such classic examples may be unusual, needing first to break a genetic lock before their beaks could evolve new shapes.

Introduction

The avian beak offers a classic example of adaptation to feeding ecology, with beak morphology frequently considered to represent evolutionary adaptation to specialised trophic niches (e.g. Galápagos finches (1); Hawaiian honeycreepers (2); Madagascan vangas (3)). Despite this axiom, we lack quantitative data on the degree to which skull and beak morphology is influenced not only by feeding ecology, but by other sources of variation or constraint (4). Although the beak is often seen as the target of selection mechanisms closely allied to feeding ecology such as prey type, feeding style, or beak use, evidence also suggests that beak morphology and variation may be constrained by a number of other factors, including evolutionary history (phylogeny) and development on the component parts of the entire skull. Breakthrough experiments in molecular genetics have shown that the mechanisms driving beak shape variation encompass modifications to the timing of expression of conserved developmental pathways (5-9), resulting in beak diversity described by a few relatively simple geometric transformations (10). However, pleiotropic associations between different skull structures can also contribute to the shape of the avian beak (11), and Sonic hedgehog signalling from the forebrain also relates to the spatial organization of, and changes to, face and beak shape (12-14). Furthermore, assessments of bird skull phenotypic variation suggest that beak morphology may evolve cohesively with cranial morphology (15, 16). Size is also an important consideration when assessing morphological variation. Larger animals generally have access to larger prey due to their increased gape and greater absolute muscular power, and size is further related to morphology via allometry, the tendency of traits to vary with size throughout a morphological structure. Allometry has been demonstrated to be a key contributing factor to craniofacial form across a range of mammalian (17, 18) and avian (15, 19) clades, and evolvability of body size is proposed to be a major evolutionary pathway in the avian stem (20).

In this study we quantify the role of adaptation versus constraint in avian craniofacial evolution. Using diurnal birds of prey (‘raptors’), we quantify the degree to which morphological convergence in feeding ecology can be attributed to variation controlled by evolutionary allometry (size), phylogeny, and integration between the beak and braincase. Raptors are an ideal group to skull avian craniofacial evolution. They possess strong, hook-shaped beaks and powerful talons for holding and tearing flesh, are found in every habitat and continent except Antarctica (21), and vary considerably in size, from 40 – 12,500 g (22). Although traditionally considered to be monophyletic, recent molecular phylogenies (23-25) recognise that diurnal raptors comprise three non-sister families: Falconidae (falcons and caracaras), Cathartidae (New-World vultures), and Accipitridae (the largest clade, including hawks, eagles, kites, harriers, buzzards, and Old-World vultures); and two further monotypic families for the osprey (Pandionidae: Pandion haliaeetus) and secretarybird (Sagittaridae: Sagittarius serpentarius). Despite some differences in the positions of Accipitridae and Falconidae between different topologies (25, 26), raptor families are consistently recovered at the base of both major landbird clades, and a raptorial ancestor for the landbird radiation has been suggested (25). Extensive

morphological and dietary convergence is seen between raptor families, for instance, between scavenging Old- and New-World Vultures (27); the avivore sparrowhawks (e.g. Accipiter nisus) and falcons (e.g. Falco columbarius); alongside the repeated evolution of recognisable ecomorphotypes (e.g. eagles, kites) within the Accipitridae (28, 29). Additionally, certain species such as the Snail Kite (Rostrhamus sociabilis) and Hook-billed Kite (Chondrohierax uncinatus) show highly specialised, independently derived beak morphologies associated with their diet.

If selection pressures underpinning raptor beak shape are related to feeding ecology, we predict that distantly related birds of the same dietary groups should share similar shaped beaks and skulls, irrespective of phylogeny (i.e. evolutionary convergence). Using 3D shape analysis, we quantify how cranial shape variation is related to size (allometry), and test the long-standing view that the beak and braincase act as independent modules, enabling birds to adapt their beaks independently to a variety of ecological roles.

Results

A three-dimensional dataset of 22 landmarks and 40 semilandmarks collected from the skulls of 147 raptor species representing all major radiations (Fig S1 and Tables S1 and S2) was subject to Procrustes superimposition and Principal Components Analysis (PCA) to generate a morphospace of skull shape variation (Fig. 1). Accipitrids and falconids occupy similar space on PC1 (59.8%, positive PC1 scores represent an elongation of the beak, flattening of the skull roof and rotation of the occipital from a ventral to a posterior orientation) (Movies S1 and S2), but separate on PC2 (11.5%, positive PC2 scores represent increased beak curvature with narrowed jugal width) (Movies S3 and S4). Permutation tests reject the null hypothesis of no phylogenetic signal ($p < 0.0001$) in skull shape. Pairwise NPMANOVA found significant differences in shape between the three main families (Bonferroni-corrected $p = 0.0003$). The two monotypic families, Pandionidae and Sagittaridae, plot within the Falconidae and Accipitridae respectively. Mapping of phylogeny over the morphospace to create a phylomorphospace reveals extensive criss-crossing of branches, yet three distinctive parallel-trending radiations stretch into sparsely populated morphospace at the positive end of PC1 (Fig. 1A): the New World cathartid vultures and the two Old World vulture accipitrid (non-sister) subfamilies, Aegypiinae and Gypaetinae. We therefore uncover an almost exclusive area of "vulture space" on PC1, with only two non-vulturine taxa falling on the very edge of this region.

Despite clustering of vultures, we find limited evidence for wholesale separation of groups on the basis of feeding ecology (Fig. 1C). Carrion feeders are statistically distinct from all other ecological groups except large vertebrate feeders, fish eaters and generalists/omnivores (Table 1), but avivores and insectivores (birds specialising in aerial prey capture) are the most distinct in the pairwise comparisons, being significantly different in seven of the eight possible pairings, but not distinct from each other. Contrary to our predictions, no dietary groups are significantly different from all the others. Piscivores are the least distinctive, with only two significantly different pairings.

The observation that birds with long beaks, and flat, narrow skulls (birds with positive PC1 values) are larger than birds with negative PC1 values was confirmed by a regression of shape data against centroid size. 47.5% of the variation in shape can be predicted from size ($p < 0.0001$), indicating a very strong allometric relationship between skull shape and size (Fig S2 A and B). The separation of vultures from other clades on PC1 therefore suggests that part of the dietary signal recovered from the morphospace is size-related (i.e., allometric), and that vultures' dietary adaptation is achieved by virtue of their increased size.

To assess the effect of allometric (size) signal in our dataset we conducted a PCA on the residuals of the regression of shape data against centroid size (henceforth R_PC). R_PC1 almost halves the variation of PC1 to represent 32.9% of the variation, but R_PC2 increases to 16.3%. When the non-allometric shape is analysed (Fig. 1 B and D), falconids and accipitrids are less distinctive but a strong phylogenetic signal is still present ($p < 0.0001$; significant pairwise NPMANOVAs between three main families (Bonferroni-corrected $p = 0.0003$)). Little separation of ecologies is apparent in the regression residuals, and there is considerable resemblance between different dietary groups. Scavengers are the most statistically distinct from the other dietary groups (Table 2), even though the two Old World vulture clades no longer radiate out to join the New World vultures in an exclusively vulturine area of morphospace.

When the landmark configurations are divided in subsets that separately outline the beak and the braincase, we find that braincase morphology is more conservative (less variable) than the beak (Fig. 2, Fig. S1, and Table S1), however both morphospaces again show significant allometric and phylogenetic signal and weak ecological clustering (Table S3-S6). Rather than acting as separate modules, we find that the beak and braincase are highly integrated structures, meaning that almost any change in beak morphology is associated with a correlated and predictable change in braincase morphology. Partial Least Squares (PLS) analysis of the beak and braincase subsets demonstrated this high degree of correlation (Fig. 2E) with PLS1 representing 97.2% of the covariation ($p < 0.001$; correlation = 0.91; RV = 0.78). Strikingly, beak-braincase covariation remains even after removal of the allometric (via regression to centroid size) or phylogenetic signal (via phylogenetic independent contrasts (30)), highlighting a conserved developmental constraint on avian craniofacial morphology (PLS1 represents 63.7% of the non-allometric covariation, $p < 0.001$, correlation = 0.79; RV = 0.48, Fig. 2F; PLS1 represents 68.0% of the non-phylogenetic covariation, $p < 0.001$, correlation = 0.88, Fig. 2G).

Shape variation associated with the original PLS1 matches the allometric trend of posterior rotation of the occipital and dorsoventral compression of the braincase with increased beak length. Using PLS and regression, we calculate the amount of integrated variation that is independent of allometry as 32.4%. Together therefore, allometry (47.5%) and integration (32.4%) predict 79.9% of the total shape variation. The remaining 20.1% still has a significant phylogenetic signal ($p < 0.0001$), but neither phylogeny nor diet form clear groups in morphospace (Fig. 3). Applying this same logic to the Phylogenetic Independent Contrasts suggests that this integration is phylogenetically conserved: a large portion of the allometric

variation is phylogenetically controlled (allometry only predicts 18.9% of the non-phylogenetic variation, instead of the 47.5% obtained earlier), but similar amounts of integration remain (27.6%).

Discussion

Beak shape is often viewed as the target for natural selection, independent of the rest of the skull (4, 31, 32). Contrary to this belief we find that in raptors, a polyphyletic group at the base of the landbird radiation, beak and braincase morphology are tightly integrated. The beak cannot evolve as a morphologically independent module; changes to beak shape result in predictable changes to braincase morphology, and vice versa. Our findings challenge the long-standing notion of the avian beak as a discrete, adaptable structure. In fact, integration of the beak and braincase, coupled to a strong allometric signal, can explain nearly 80% of skull shape variation. Moreover, this pattern of predictable skull shape changes is shared by all the families studied, pointing towards an underlying developmental control (33), and a deep, pervasive evolutionary origin for regulatory controls on bird beak shape. Our major axes of beak shape variation (long and narrow vs. short and wide) parallel changes to beak shape in finches linked to signalling molecules such as calmodulin (7) and bone morphogeneic protein 4 (BMP4) (6, 8).

We find a strong relationship between skull shape and size, showing that size is an effective mechanism by which raptors may modify their feeding ecology. For example, niche partitioning and adaptation to certain diets, such as carrion or aerial prey capture, is achieved by changes to body size and subsequently skull size, with the resulting shape being constrained and defined by the nature of beak-braincase integration. However, at body masses above ~3 kg, skull size and shape plateaus (Fig. S2B and C), indicating a constraint on maximum head size. The analyses show that all vultures look alike in spite of their different ancestry. Although the vulture clades do not completely converge in shape, this clustering of non-sister taxa based on diet (after (34, 35)) is strong evidence for “incomplete convergence” (36, 37), as has been recognised in other animal groups (e.g. lizards (38)). Taxa that capture aerial prey (insects and birds) are distinct from many other ecological groups, but no ecological grouping is significantly different from all others. A number of raptors are generalist opportunist predators, and will vary their diets in order to reflect prey availability (21), thus perhaps limiting the extent to which the skull can afford to be morphologically specialised towards particular prey. Other behavioural factors, such as hunting strategy (e.g. sit-and-wait vs. aerial pursuit) may also exert an influence on skull morphology. Birds have highly mobile skulls comprised of multiple parts that are able to move during feeding including a flexible region, or ‘hinge’, separating the beak and braincase into two kinetic modules (32, 39, 40). Despite generating beak movement, the adductor muscles never exert force directly on to the upper beak. Further research is therefore warranted to investigate whether biomechanical function is similarly integrated (41), and how the shape of the upper beak is affected by the skull musculature as it develops. Finally, the phenomena of ‘many-to-one’ and ‘one-to-many’ mapping between form and function mean that similarities in shape do not

necessarily imply similarity in function (42-44), further justifying the need for biomechanical analyses of avian skulls.

Evolutionary history plays a significant role in dictating skull shape. Statistically the accipitrids, falconids and cathartids are morphologically distinct, despite some overlap in morphospace. Further, a strong phylogenetic signal is observed in the beak as well as in the braincase, despite the fact that the beak should intuitively be the target of intense selection pressure towards convergence due to its role in feeding. This result undoubtedly reflects the strong integration observed between the beak and braincase. The considerable crossing of clades over morphospace indicates low disparity of forms relative to the number of species (45), indicating that raptors are thoroughly exploring a tightly-constrained morphological space, either through extensive convergence, or alternatively, limited shape change from a basal morphological state.

The shape change associated with beak-cranium integration mirrors that of allometry, although size alone does not explain this trend, and phylogeny plays a key role. The trend for the face to elongate with allometry has also been noted in mammals (17), and is postulated to be related to heterochrony, an important factor in the evolution of birds from dinosaurs (46) and a demonstrated mode of generating diversity of beak forms in Darwin's finches (6, 9). In mammals, it has been shown that integration constrains evolution along paths of least evolutionary resistance, meaning that heterochronic or allometric changes offer a simple mechanism by which evolution can act to produce high disparity (47, 48). The fact that two non-sister clades of accipitrid vultures achieve a vulturine-morphology solely by increasing skull size provides a new, non-mammalian example of this phenomenon. A consequence of this mechanism is that skull morphology is highly constrained. Interestingly, animals that demonstrate high levels of integration are less able to respond to shifting selective pressures because they are locked in to a particular dimensions of variation (47, 49), in this case, size. Consequently, raptors may be particularly vulnerable if changing environmental conditions result in an adaptive peak that they cannot reach by simply sliding along their allometric trajectory.

Our study was conducted across a polyphyletic group bracketing the base of the landbird radiation. Regardless of whether raptors occur at the base of two major radiations of monophyletic landbirds (25), or if Accipitridae are found at the base of all landbirds with Falconidae sister to the parrots and Passeriformes (26), it raises the question of whether integration and allometric control on form is basal to landbirds, or has been independently acquired in all raptorial groups from a modular plesiomorphic condition. Given that integration accounts for the same proportion of the variation in the original shape data as in the phylogenetically controlled dataset, we believe that beak-braincase integration as basal to the landbird radiation is the most parsimonious explanation. However, in order to confirm this hypothesis, more data are needed from other landbirds. Widespread beak-braincase integration has significant ramifications for the notion that bird beaks are independent agents of selection and adaptation, and raises the possibility that release from this constraint is a necessary precursor

to facilitate classic 'textbook' avian adaptive radiations such as finches, vangas, and Hawaiian honeycreepers.

Materials and Methods:

Fourteen landmarks were collected from the midline and left-hand side of the beaks and braincases of 147 raptor species, representing all the major radiations (Fig. S1 and Tables S1 and S2), using a MicroScribe G2LX digitiser (Revware Systems, Inc., San Jose, CA). These landmarks were then reflected along the midline landmarks and realigned using FileConverter (http://www.flywings.org.uk/fileConverter_page.htm) to give 22 landmarks in total. Surfaces of the same specimens were obtained using a NextEngine laser scanner and MultiDrive running ScanStudio HD Pro 1.3.2 (NextEngine, Inc. Santa Monica, CA) or with digital photogrammetry (Photoscan 0.9.0, AgiSoft, Russia), and were used to place landmarks along the dorsal margins of the beak and braincase, and bilaterally on the tomial edges of the beak in HyperMesh 11.0 (Altair Engineering Inc., Troy, MI). Landmarks were then resampled (resample.exe; http://life.bio.sunysb.edu/morph/soft-utility.html) to give 10 equally spaced semilandmarks along each curve. Specimens without a keratinous rhamphotheca were selected, as this preparation is most commonly found in museum collections. All data was collected during a single visit to the Smithsonian Institution National Museum of Natural History.

The 62 landmarks and semilandmarks were collated for each specimen, and the semilandmarks were slid to minimise bending energy in the Geomorph package for R (43). The slid configurations for all birds were then imported to MorphoJ (44) and subjected to a Procrustes Superimposition. Principle Components Analysis (PCA) was used to explore shape variation within the sample. The skull of a common buzzard (Buteo buteo) was CT scanned (X-Tek HMX 160 μCT system at the University of Hull, 0.0581 mm resolution, 95 kV, 60 μA) and the bones were segmented in Avizo (version 7.0, Visualization Science Group). The resulting surface was landmarked in Avizo, and used to create warps of the maximum and minimum PC scores in all morphospaces using the plotRefToTarget function in Geomorph based on the PC scores from MorphoJ. Significant morphological differences were assessed by Euclidean NPMANOVA to the Principal Component (PC) scores across all PCs (PAST 2.17; (45)), between the three largest families. Pandionidae and Sagittaridae were excluded from these analyses as each had only one representative, invalidating the sample size criteria of the statistical tests (Table S1). Each species was also assigned to one of ten dietary categories based on their preferred prey as determined from (21) (Table S2). NPMANOVA was performed using these groupings to determine significant morphological differences between birds with different dietary preferences (Table 1). Birds of unknown dietary preference were excluded from these analyses.

A maximum clade credibility tree of the species in the analysis was constructed from a set of 1,000 molecular trees ((24); www.birdtree.org) using the TreeAnnotator package in BEAST

2.1.2 ((46); Fig. S3). This phylogeny was mapped on to the PC scores in MorphoJ using unweighted square-change parsimony (47), and a permutation test for phylogenetic signal was performed over 10,000 iterations. The Phytools package in R (48) was used to generate a phylomorphospace based on the PC scores from MorphoJ.

After noticing that position on PC1 appeared to be correlated with size, the symmetric component of shape variation was regressed in MorphoJ on to the centroid sizes of the specimens (Fig. S2A), and on to an estimate of body mass (Fig. S2B) taken from (22). Body mass estimates were not available for some species (Table S2), so these species were excluded from the regression to body mass. Significance was assessed over 10,000 permutations ($p < 0.0001$) in both regressions.

To assess the effects of size-related variation in shape (allometry) on our results, all analyses were repeated on the residuals of the regression to centroid size. NPMANOVA results for dietary differences in Table 2.

The landmark configuration was separated into two subsets (blocks) representing the beak and braincase (Fig S1), and morphospaces were generated for each block independently (Fig. 2 A-D). The degree of covariation between the two blocks was assessed over 250 permutations using two-block within-configuration Partial Least Squares (PLS) Analysis in MorphoJ (Fig. 2E). This analysis was also repeated on the regression residuals to see how the two blocks covaried in the absence of allometry (Fig. 2F). NPMANOVA of the PC scores of both the beak and the braincase individually gave similar results to the whole skull (Tables S3-S6).

Phylogenetic Independent Contrasts (PICs; (29)) were calculated in MorphoJ in order to remove the aspects of shape associated with relatedness. The PLS analysis was repeated on the PICs in order to assess whether covariation was associated with phylogenetic structure (Fig. 2G).

Partial Least Squares only evaluates the amount of covariation, but it does not make any assessment of the amount of overall variation explained by the covariation. In order to determine how much of the non-allometric shape (the residuals from the regression of the original shape data to centroid size) was explained by the covariation between the braincase and the beak, we first regressed the PLS1 scores of the non-allometric data (which explained 63.7% of the covariation) of Block 1 against the non-allometric PLS1 Block 2 to obtain an eigenvector for the non-allometric PLS1. The predication of this regression was then itself regressed against the the non-allometric shape to give the non-allometric, non-integrated shape data (representing 32.4% of the overall variation) presented in Fig. 3. This same method was applied to the PICs to assess the degree to which these relationships were affected by relatedness.

Acknowledgments:

Chris Milensky at the Smithsonian Institution National Museum of Natural History, and Jo Cooper and Judith White at Natural History Museum, Tring, are thanked for providing access to

specimens. CT scanning for morphometric warps was provided by Michael Fagan and Sue Taft (University of Hull). Funding was provided by BBSRC grants BB/I011668/1 and BB/I011714/1.

References

1. Grant BR & Grant PR (1993) Evolution of Darwin's Finches Caused by a Rare Climatic Event. Proceedings of the Royal Society B: Biological Sciences 251(1331):111-117.
2. Lovette IJ, Bermingham E, & Ricklefs RE (2002) Clade-specific morphological diversification and adaptive radiation in Hawaiian songbirds. Proc Biol Sci 269(1486):37-42.
3. Jønsson KA, et al. (2012) Ecological and evolutionary determinants for the adaptive radiation of the Madagascan vangas. Proc Natl Acad Sci U S A 109(17):6620-6625.
4. Zusi RL (1993) Patterns of Diversity in the Avian Skull. The Skull, Volume 2: Patterns of Structural and Systematic Diversity, eds Hanken J & Hall BK (The University of Chicago Press, Chicago, USA), Vol 2, pp 391-437.
5. Schneider RA & Helms JA (2003) The cellular and molecular origins of beak morphology. Science 299:565-568.
6. Abzhanov A, Protas M, Grant BR, Grant PR, & Tabin CJ (2004) Bmp4 and morphological variation of beaks in Darwin's finches. Science 305(5689):1462-1465.
7. Abzhanov A, et al. (2006) The calmodulin pathway and evolution of elongated beak morphology in Darwin's finches. Nature 442(7102):563-567.
8. Wu P, Jiang TX, Shen JY, Widelitz RB, & Chuong CM (2006) Morphoregulation of avian beaks: comparative mapping of growth zone activities and morphological evolution. Dev Dyn 235(5):1400-1412.
9. Mallarino R, et al. (2011) Two developmental modules establish 3D beak-shape variation in Darwin's finches. Proc Natl Acad Sci U S A 108(10):4057-4062.
10. Fritz JA, et al. (2014) Shared developmental programme strongly constrains beak shape diversity in songbirds. Nat Commun 5:3700.
11. Bhullar BA, et al. (2015) A molecular mechanism for the origin of a key evolutionary innovation, the bird beak and palate, revealed by an integrative approach to major transitions in vertebrate history. Evolution 69(7):1665-1677.
12. Marcucio RS, Cordero DR, Hu D, & Helms JA (2005) Molecular interactions coordinating the development of the forebrain and face. Dev Biol 284(1):48-61.
13. Young NM, Chong HJ, Hu D, Hallgrímsson B, & Marcucio RS (2010) Quantitative analyses link modulation of sonic hedgehog signaling to continuous variation in facial growth and shape. Development 137(20):3405-3409.
14. Hu D, et al. (2015) Signals from the brain induce variation in avain facial shape. Developmental Dynamics 244 (9):1133-1143.
15. Kulemeyer C, Asbahr K, Gunz P, Frahnert S, & Bairlein F (2009) Functional morphology and integration of corvid skulls - a 3D geometric morphometric approach. Front Zool 6:2.
16. Klingenberg CP & Marugán-Lobón J (2013) Evolutionary covariation in geometric morphometric data: analyzing integration, modularity, and allometry in a phylogenetic context. Syst Biol 62(4):591-610.
17. Cardini A & Polly PD (2013) Larger mammals have longer faces because of size-related constraints on skull form. Nat Commun 4:2458.

18. Singh N, Harvati K, Hublin JJ, & Klingenberg CP (2012) Morphological evolution through integration: a quantitative study of cranial integration in Homo, Pan, Gorilla and Pongo. J Hum Evol 62(1):155-164.
19. Marugán-Lobón J & Buscalioni ÁD (2004) Geometric morphometrics in macroevolution: morphological diversity of the skull in modern avian forms in contrast to some theropod dinosaurs. Morphometrics: Applications in Biology and Palaeontology, ed Elewa AMT (Springer-Verlag, New York, USA), pp 157-173.
20. Benson RB, et al. (2014) Rates of dinosaur body mass evolution indicate 170 million years of sustained ecological innovation on the avian stem lineage. PLoS Biol 12(5):e1001853.
21. del Hoyo J, Elliott A, & Sargatal J (1994) New World Vultures to Guineafowl, Handbook of Birds of the World (Lynx Edicions, Barcelona), Vol 2.
22. Dunning Jr. JB (1993) CRC Handbook of Avian Body Masses (CRC Press, Florida, USA).
23. Hackett SJ, et al. (2008) A phylogenomic study of birds reveals their evolutionary history. Science 320(5884):1763-1768.
24. Jetz W, Thomas GH, Joy JB, Hartmann K, & Mooers AO (2012) The global diversity of birds in space and time. Nature 491(7424):444-448.
25. Jarvis ED, et al. (2014) Whole-genome analyses resolve early branches in the tree of life of modern birds. Science 346(6215):1320-1331.
26. Prum RO, et al. (2015) A comprehensive phylogeny of birds (Aves) using targeted next-generation DNA sequencing. Nature 526(7574):569-573.
27. Hertel F (1994) Diversity in body size and feeding morphology within past and present vulture assemblages. Ecology 75(4):1074-1084.
28. Lerner HR & Mindell DP (2005) Phylogeny of eagles, Old World vultures, and other Accipitridae based on nuclear and mitochondrial DNA. Mol Phylogenet Evol 37(2):327-346.
29. Griffiths CS, Barrowclough GF, Groth JG, & Mertz LA (2007) Phylogeny, diversity, and classification of the Accipitridae based on DNA sequences of the RAG-1 exon. J Avian Biol 38(5):587-602.
30. Felsenstein J (1985) Phylogenies and the comparative method. Am Nat 125(1):1-15.
31. Zusi RL (1967) The role of the depressor mandibulae muscle in kinesis of the avian skull. Proceedings of the United States National Museum 123 (3607):1-28.
32. Beecher WJ (1962) The bio-mechanics of the bird skull. Bulletin of the Chicago Academy of Sciences 11 (2):10-33.
33. Hallgrímsson B, et al. (2009) Deciphering the Palimpsest: Studying the Relationship Between Morphological Integration and Phenotypic Covariation. Evol Biol 36(4):355-376.
34. Hertel F (1995) Ecomorphological indicators of feeding behavior in recent and fossil raptors. The Auk 112(4):890-903.
35. Si G, Dong Y, Ma Y, & Zhang Z (2015) Shape similarities and differences in the skulls of scavenging raptors. Zoolog Science 32(2):171-177.
36. Herrel A, Vanhooydonck B, & Van Damme R (2004) Omnivory in lacertid lizards: adaptive evolution or constraint? J Evol Biol 17(5):974-984.
37. Losos JB (2011) Convergence, adaptation, and constraint. Evolution 65(7):1827-1840.

38. Stayton CT (2006) Testing hypotheses of convergence with multivariate data: morphological and functional convergence among herbivorous lizards. Evolution 60(4):824-841.
39. Gussekloo SW & Bout RG (2005) Cranial kinesis in palaeognathous birds. J Exp Biol 208(Pt 17):3409-3419.
40. Dawson MM, Metzger KA, Baier DB, & Brainerd EL (2011) Kinematics of the quadrate bone during feeding in mallard ducks. J Exp Biol 214(Pt 12):2036-2046.
41. Klingenberg CP (2014) Studying morphological integration and modularity at multiple levels: concepts and analysis. Philos Trans R Soc Lond B Biol Sci 369(1649):20130249.
42. Lauder GV (1995) On the inference of function from structure. Functional Morphology in Vertebrate Paleontology, ed Thomason JJ (Cambridge University Press, Cambridge, UK), pp 1-18.
43. Anderson PS, Friedman M, Brazeau MD, & Rayfield EJ (2011) Initial radiation of jaws demonstrated stability despite faunal and environmental change. Nature 476(7359):206-209.
44. Stubbs TL, Pierce SE, Rayfield EJ, & Anderson PS (2013) Morphological and biomechanical disparity of crocodile-line archosaurs following the end-Triassic extinction. Proc Biol Sci 280(1770):20131940.
45. Sidlauskas B (2008) Continuous and arrested morphological diversification in sister clades of characiform fishes: a phylomorphospace approach. Evolution 62(12):3135-3156.
46. Bhullar BA, et al. (2012) Birds have paedomorphic dinosaur skulls. Nature 487(7406):223-226.
47. Marroig G, Shirai LT, Porto A, de Oliveira FB, & De Conto V (2009) The Evolution of Modularity in the Mammalian Skull II: Evolutionary Consequences. Evol Biol 36(1):136-148.
48. Goswami A, Smaers JB, Soligo C, & Polly PD (2014) The macroevolutionary consequences of phenotypic integration: from development to deep time. Philos Trans R Soc Lond B Biol Sci 369(1649):20130254.
49. Villmoare B (2012) Morphological Integration, Evolutionary Constraints, and Extinction: A Computer Simulation-Based Study. Evolutionary Biology 40(1):76-83.

Figure legends:

Fig. 1. Principal Components Analyses of raptor skulls. Phylomorphospaces of the original (A) and non-allometric (B) shape data, coloured to indicate family (two Accipitrid subfamilies of Old World vulture are also highlighted). Morphospaces of the original (C) and non-allometric (D) shape data, coloured to indicate dietary preference.

Fig. 2. Relationship between the beak and braincase. Phylomorphospaces of the beak (A) and braincase (B) individually, coloured to indicate family (two Accipitrid subfamilies of Old World vulture are also highlighted). Morphospaces of the beak (C) and braincase (D) individually, coloured to indicate dietary preference. Partial Least Squares analyses showing covariation

between the beak and braincase blocks in the original shape data (E), the non-allometric shape data (F), and the phylogenetic independent contrasts (G).

Fig. 3. Variation remaining when allometry and integration are removed. A) Phylomorphospace coloured to indicate family (two Accipitrid subfamilies of Old World vulture are also highlighted). B) Morphospace coloured to indicate dietary preference.

Figures

Fig. 1.

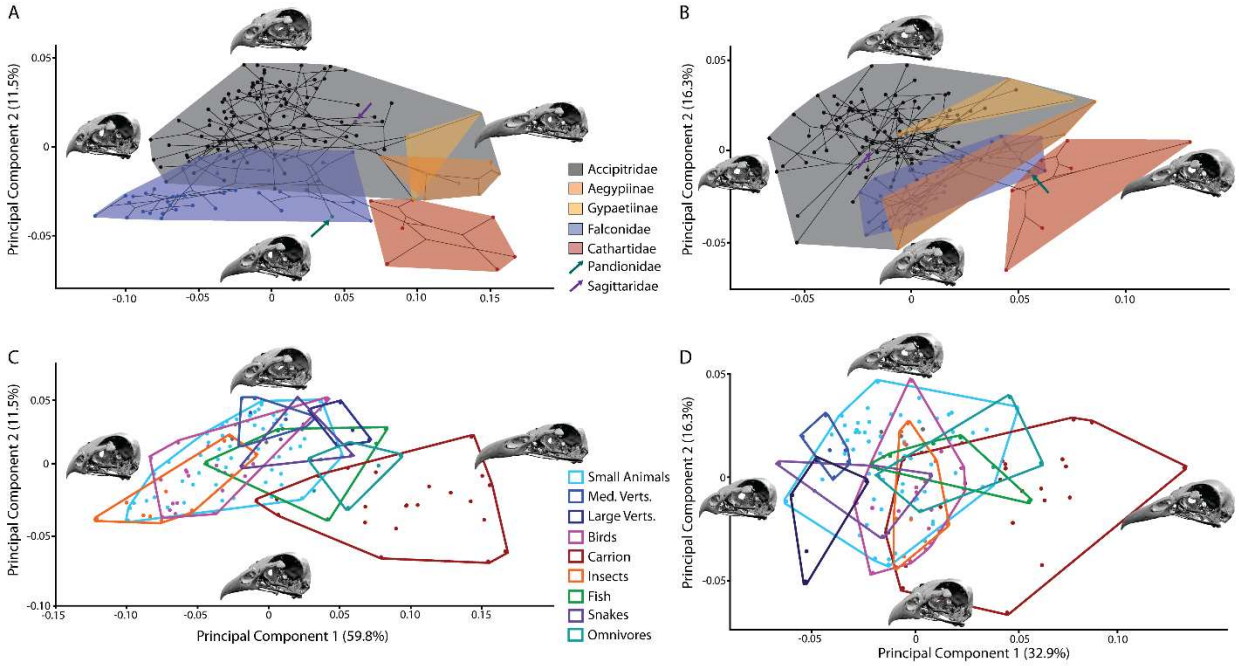

Fig. 2.

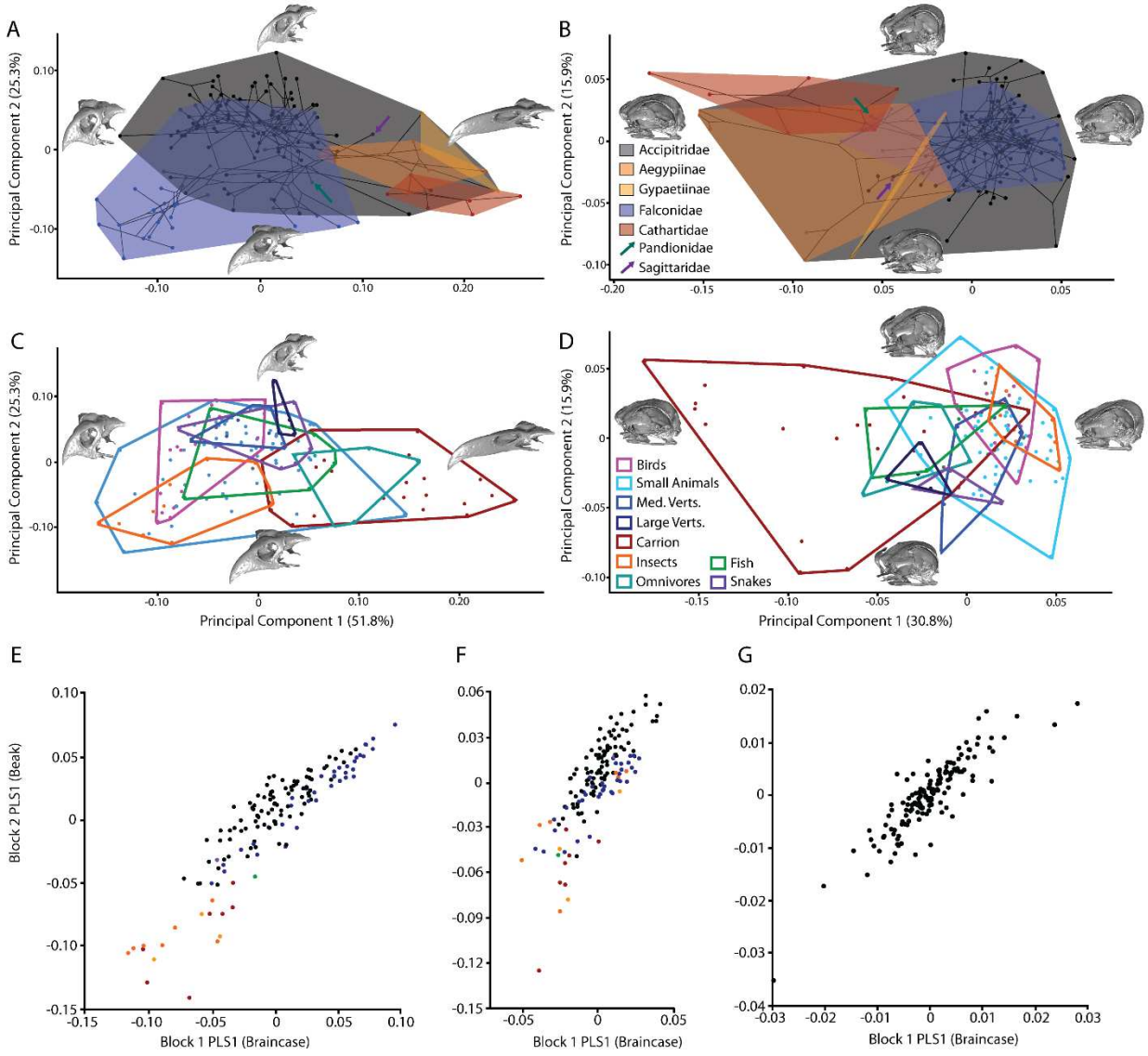
A
B
C
D
E
F
G
Principal Component 2 (25.3%)
Principal Component 2 (15.9%)
Principal Component 1 (51.8%)
Principal Component 1 (30.8%)
Accipitridae
Aegypiinae
Gypaetiinae
Falconidae
Cathartidae
Pandionidae
Sagittaridae
Birds
Small Animals
Med. Verts.
Large Verts.
Carrion
Insects
Omnivores
Fish
Snakes
Block 2 PLS1 (Beak)
Block 1 PLS1 (Braincase)

Fig. 3.

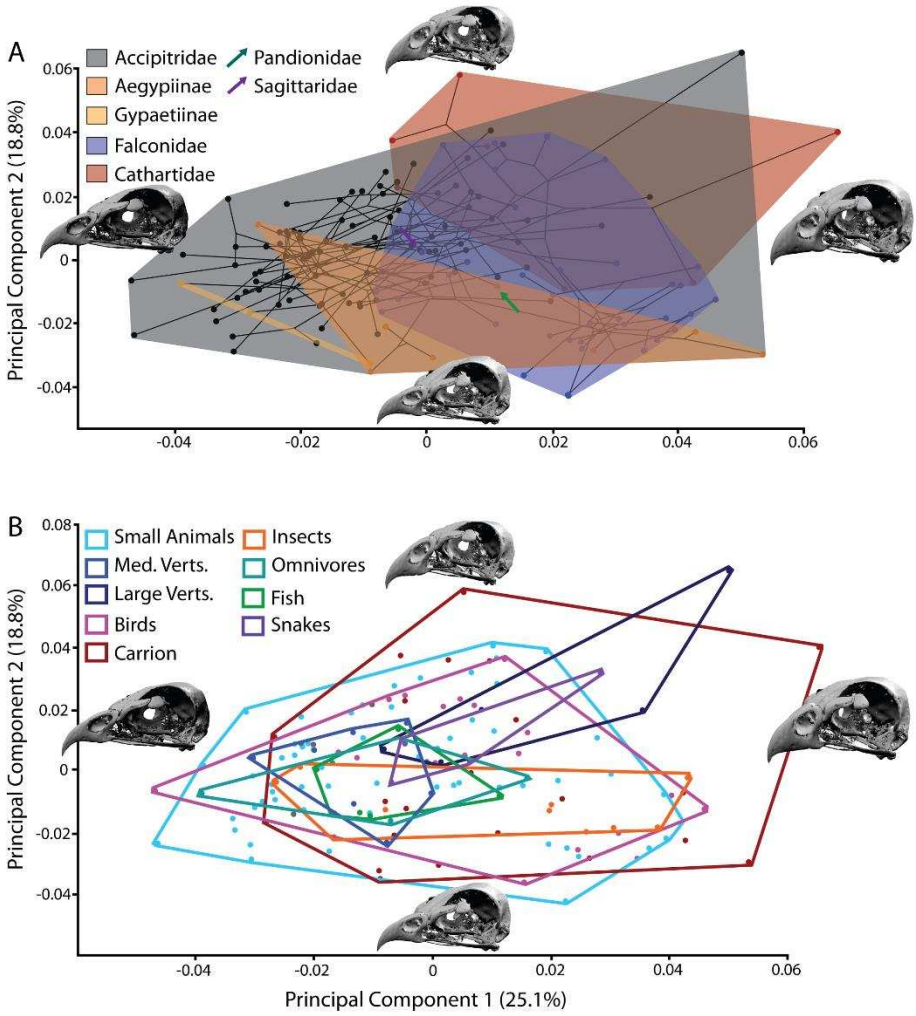
A
Accipitridae
Aegypiinae
Gypaetiinae
Falconidae
Cathartidae
Pandionidae
Sagittaridae
Principal Component 2 (18.8%)
0.06
0.04
0.02
0
-0.02
-0.04
-0.04
-0.02
0
0.02
0.04
0.06
B
Small Animals
Med. Verts.
Large Verts.
Birds
Carrion
Insects
Omnivores
Fish
Snakes
Principal Component 2 (18.8%)
0.08
0.06
0.04
0.02
0
-0.02
-0.04
-0.04
-0.02
0
0.02
0.04
0.06
Principal Component 1 (25.1%)

Tables

Table 1. Euclidean NPMANOVA of PC scores, with Bonferroni-corrected p-values showing differences between dietary groups. Bold values indicate significantly different pairings ($p < 0.05$).

	Small Animals	Medium Vertebrates	Large Vertebrates	Birds	Carrion	Insects	Fish	Snakes	Generalist/ Omnivore
Small Animals		1	**0.0036**	**0.0144**	**0.0036**	**0.018**	0.0504	0.72	**0.0036**
Medium Vertebrates	1		0.0792	**0.0036**	**0.0036**	**0.0144**	1	1	**0.0216**
Large Vertebrates	**0.0036**	0.0792		**0.0036**	0.1152	**0.0108**	0.8172	1	0.1728
Birds	**0.0144**	**0.0036**	**0.0036**		**0.0036**	1	**0.0252**	**0.0216**	**0.0036**
Carrion	**0.0036**	**0.0036**	0.1152	**0.0036**		**0.0036**	0.342	**0.0252**	1
Insects	**0.018**	**0.0144**	**0.0108**	1	**0.0036**		**0.0252**	**0.0252**	**0.0072**
Fish	0.0504	1	0.8172	**0.0252**	0.342	**0.0252**		1	1
Snakes	0.72	1	1	**0.0216**	**0.0252**	**0.0252**	1		0.6444
Generalist/ Omnivore	**0.0036**	**0.0216**	0.1728	**0.0036**	1	**0.0072**	1	0.6444	

Table 2. Euclidean NPMANOVA of regression residuals' PC scores, with Bonferroni-corrected p-values showing differences between dietary groups. Bold values indicate significantly different pairings ($p < 0.05$).

	Small Animals	Medium Vertebrates	Large Vertebrates	Birds	Carrion	Insects	Fish	Snakes	Generalist/ Omnivore
Small Animals		0.2988	**0.0108**	**0.0108**	**0.0036**	0.054	1	1	0.0648
Medium	0.2988		0.3384	**0.0036**	**0.0036**	**0.0036**	**0.018**	1	**0.036**

Vertebrates									
Large Vertebrates	**0.0108**	0.3384		**0.0144**	**0.0036**	**0.0108**	0.1584	1	0.1188
Birds	**0.0108**	**0.0036**	**0.0144**		**0.0036**	0.1944	0.9036	0.1008	**0.0108**
Carrion	**0.0036**	**0.0036**	**0.0036**	**0.0036**		**0.0072**	0.7668	**0.0036**	1
Insects	0.054	**0.0036**	**0.0108**	0.1944	**0.0072**		0.2556	0.252	0.0612
Fish	1	**0.018**	0.1584	0.9036	0.7668	0.2556		0.5904	1
Snakes	1	1	1	0.1008	**0.0036**	0.252	0.5904		1
Generalist/ Omnivore	0.0648	**0.036**	0.1188	**0.0108**	1	0.0612	1	1	

The shapes of bird beaks are highly controlled by non-dietary factors

Jen Bright, Jesús Marugán-Lobón, Sam Cobb, Emily Rayfield

Suppplementary Information

Fig. S1

Buteo buteo showing landmarks and semilandmark curves used in analysis. Black = "beak" block, Blue = "braincase" block.

Fig. S2

Tree used in phylomorphospace analyses. Black = Accipitridae [Orange = Accipitridae: Gypaetiinae (Old World Vultures); Yellow = Accipitridae: Aegypiinae (Old World Vultures)]; Blue = Falconidae; Red = Cathartidae (New World Vultures); Green = Pandionidae (Osprey); Purple = Sagittaridae (Secretarybird).

Fig. S3

A) Regression of the symmetric component of shape change to centroid size. B) Regression of the symmetric component of shape change to estimated body mass. C) Regression of centroid size to estimated body mass. Black = Accipitridae [Orange = Accipitridae: Gypaetiinae (Old World Vultures); Yellow = Accipitridae: Aegypiinae (Old World Vultures)]; Blue = Falconidae; Red = Cathartidae (New World Vultures); Green = Pandionidae (Osprey); Purple = Sagittaridae (Secretarybird).

Movie S1

Animation showing shape changes along PC1, in a left lateral view.

Movie S2

Animation showing shape changes along PC1, in a dorsal view.

Movie S3

Animation showing shape changes along PC2, in a left lateral view.

Movie S4

Animation showing shape changes along PC2, in a dorsal view.

Supplementary Figures

Fig. S1

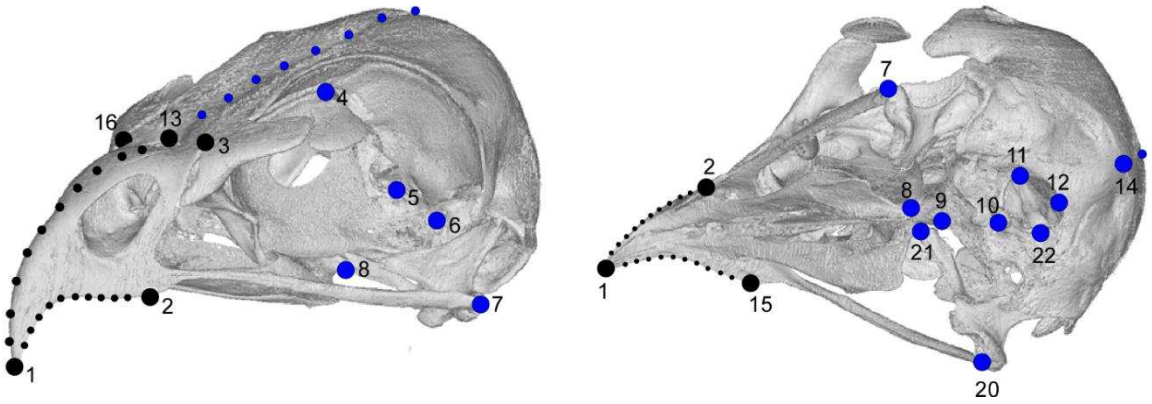

Fig. S2

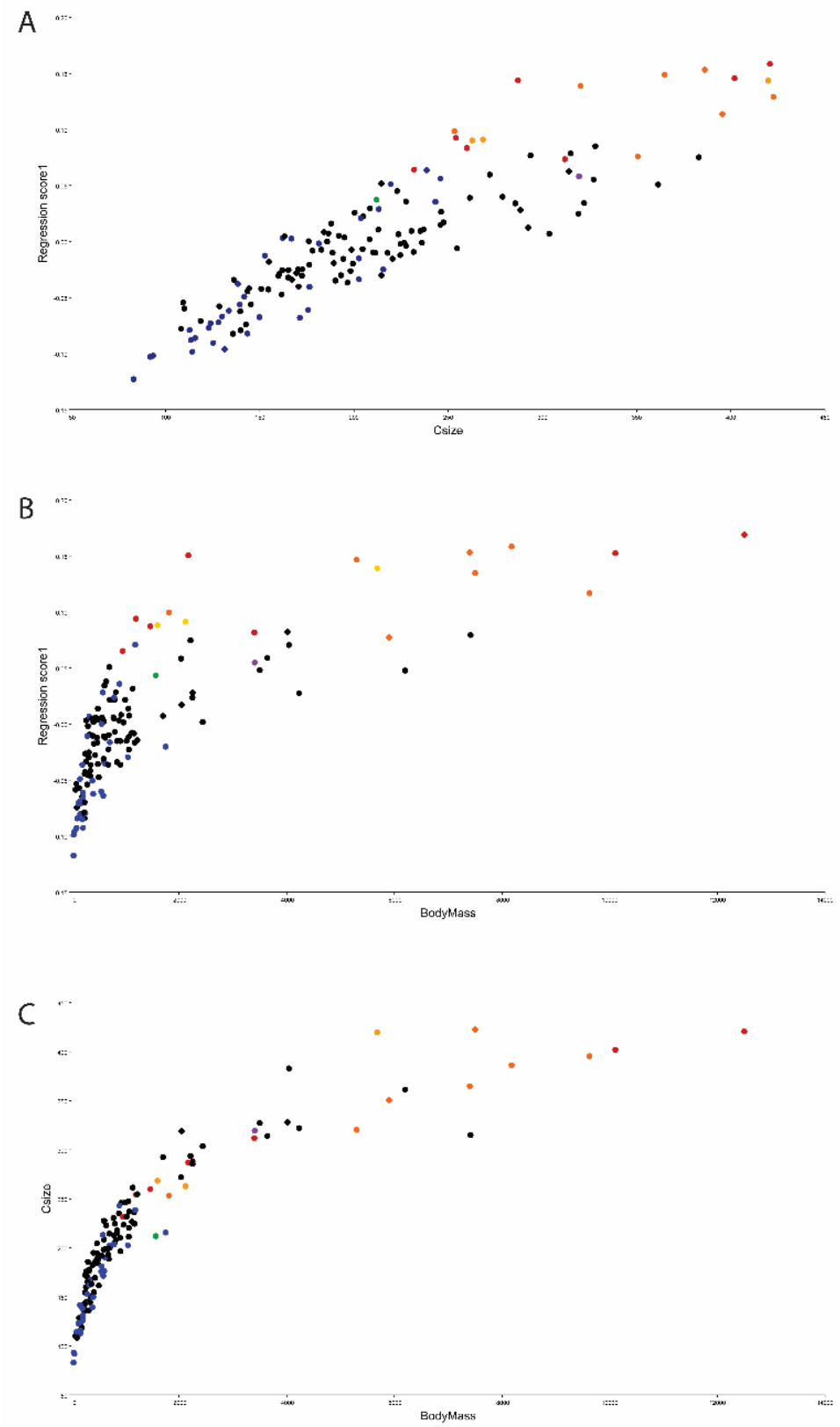
A
Regression score1
Csize
B
Regression score1
BodyMass
C
Csize
BodyMass

Fig. S3.

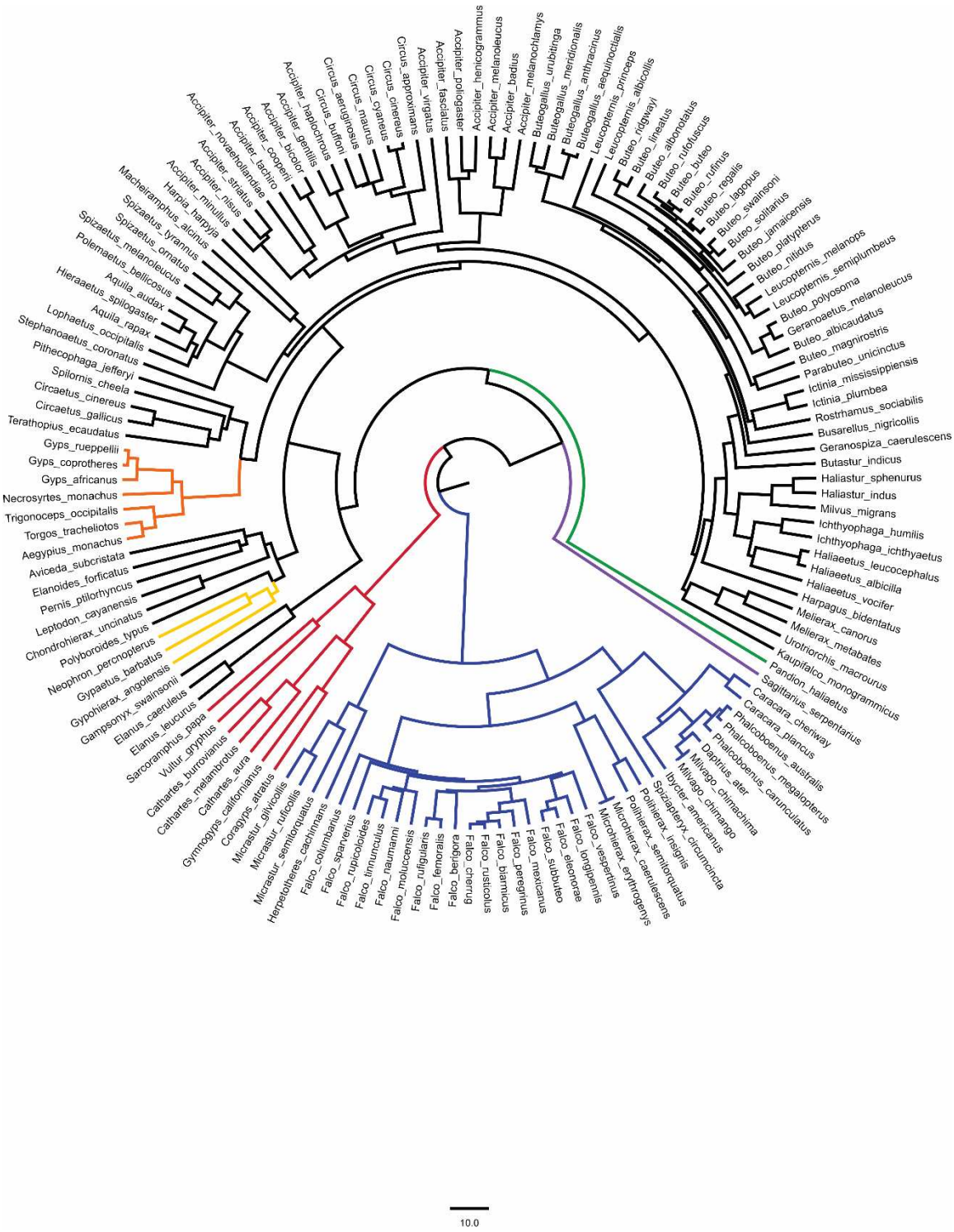
Accipiter_henicogrammus
Accipiter_poliogaster
Accipiter_fasciatus
Accipiter_virgatus
Circus_approximans
Circus_cinereus
Circus_cyaneus
Circus_maurus
Circus_aeruginosus
Circus_buffoni
Accipiter_haplochrous
Accipiter_gentilis
Accipiter_bicolor
Accipiter_cooperii
Accipiter_tachiro
Accipiter_novaehollandiae
Accipiter_striatus
Accipiter_nisus
Accipiter_minullus
Harpia_harpyja
Spizaetus_alcinus
Spizaetus_tyrannus
Spizaetus_ornatus
Spizaetus_melanoleucus
Polemaetus_bellicosus
Aquila_audax
Aquila_rapax
Hieraaetus_spilogaster
Lophaetus_occipitalis
Stephanoaetus_coronatus
Pithecophaga_jefferyi
Spilornis_cheela
Circaetus_cinereus
Circaetus_gallicus
Terathopius_ecaudatus
Gyps_rueppellii
Gyps_coprotheres
Gyps_africanus
Necrosyrtes_monachus
Trigonoceps_occipitalis
Torgos_tracheliotos
Aegypius_monachus
Aviceda_subcristata
Elanoides_forficatus
Pernis_ptilorhyncus
Leptodon_cayanensis
Chondrohierax_uncinatus
Polyboroides_typus
Neophron_percnopterus
Gypaetus_barbatus
Gypohierax_angolensis
Gampsonyx_swainsonii
Elanus_caeruleus
Elanus_leucurus
Sarcoramphus_papa
Vultur_gryphus
Cathartes_burrovianus
Cathartes_melambrotus
Cathartes_aura
Coragyps_californianus
Gymnogyps_californianus
Micrastur_gilvicollis
Micrastur_ruficollis
Micrastur_semitorquatus
Herpetotheres_cachinnans
Falco_columbarius
Falco_sparverius
Falco_rupicoloides
Falco_tinnunculus
Falco_naumanni
Falco_moluccensis
Falco_rufigularis
Falco_femoralis
Falco_berigora
Falco_cherrug
Falco_rusticolus
Falco_biarmicus
Falco_peregrinus
Falco_mexicanus
Falco_subbuteo
Falco_eleonorae
Falco_longipennis
Falco_vespertinus
Microhierax_erythrogenys
Microhierax_caerulescens
Polihierax_semitorquatus
Polihierax_insignis
Spiziapteryx_circumcincta
Ibycter_americanus
Milvago_chimango
Milvago_chimachima
Daptrius_ater
Phalcoboenus_carunculatus
Phalcoboenus_megalopterus
Phalcoboenus_australis
Caracara_plancus
Caracara_cheriway
Sagittarius_serpentarius
Pandion_haliaetus
Kaupifalco_monogrammicus
Urotriorchis_macrourus
Melierax_metabates
Melierax_canorus
Harpagus_bidentatus
Haliaeetus_vocifer
Haliaeetus_albicilla
Haliaeetus_leucocephalus
Haliaeetus_ichthyaetus
Ichthyophaga_ichthyaetus
Ichthyophaga_humilis
Milvus_migrans
Haliastur_indus
Haliastur_sphenurus
Butastur_indicus
Geranospiza_caerulescens
Busarellus_nigricollis
Rostrhamus_sociabilis
Ictinia_plumbea
Ictinia_mississippiensis
Parabuteo_unicinctus
Buteo_magnirostris
Buteo_albicaudatus
Geranoaetus_melanoleucus
Buteo_polyosoma
Leucopternis_semiplumbeus
Leucopternis_melanops
Buteo_nitidus
Buteo_platypterus
Buteo_jamaicensis
Buteo_solitarius
Buteo_swainsoni
Buteo_lagopus
Buteo_regalis
Buteo_rufinus
Buteo_buteo
Buteo_rufofuscus
Buteo_albonotatus
Buteo_lineatus
Buteo_ridgwayi
Leucopternis_albicollis
Leucopternis_princeps
Leucopternis_aequinoctialis
Buteogallus_anthracinus
Buteogallus_meridionalis
Buteogallus_urubitinga
Buteogallus_coronatus
Accipiter_melanochlamys
Accipiter_badius
Accipiter_melanoleucus
10.0

Supplementary Tables

Table S1.

Landmark list and semilandmark curves (L = left hand side, R = right hand side, CN = cranial nerve)

Landmark	Location	Block
LM1	Tip of the beak	Beak
LM2	Anteriormost position of antorbital fenestra, projected perpendicular to the tomial edge (L)	Beak
LM3	Centre of the craniofacial hinge, projected perpendicular to the lacrimal articulation (L)	Beak
LM4	Anteriormost point of the olfactory nerve (CN 1) opening (L)	Braincase
LM5	Lateralmost point of the trigeminal nerve (CN V) opening (L)	Braincase
LM6	Lateralmost point of the facial nerve (CN VII) opening (L)	Braincase
LM7	Articulation between jugal and quadrate (L)	Braincase
LM8	Articulation between palatine and pterygoid (L)	Braincase
LM9	Centre of nuchal crest	Braincase
LM10	Centre of occipital condyle	Braincase
LM11	Lateralmost point of foramen magnum (L)	Braincase
LM12	Posteriormost point of foramen magnum	Braincase
LM13	Centre of craniofacial hinge	Beak
LM14	Centre of nuchal crest	Braincase
LM15	Anteriormost position of antorbital fenestra, projected perpendicular to the tomial edge (R)	Beak
LM16	Centre of the craniofacial hinge, projected perpendicular to the lacrimal articulation (R)	Beak
LM17	Anteriormost point of the olfactory nerve (CN 1) opening (R)	Braincase
LM18	Lateralmost point of the trigeminal nerve (CN V) opening (R)	Braincase
LM19	Lateralmost point of the facial nerve (CN VII) opening (R)	Braincase
LM20	Articulation between jugal and quadrate (R)	Braincase
LM21	Articulation between palatine and pterygoid (R)	Braincase
LM22	Lateralmost point of foramen magnum (R)	Braincase
Curve 1	Dorsal profile of beak, between landmarks 1-13	Beak
Curve 2	Dorsal profile of braincase, between landmarks 13-14	Braincase
Curve 3	Left tomial edge, between landmarks 1-2	Beak
Curve 4	Right tomial edge, between landmarks 1-15	Beak

Table S2.
Specimens used in analysis.

Scientific name	Family	Diet	Sex	Mass (g)*	NMNH Specimen #	Surface
Accipiter badius polyzonoides	Accipitridae	Small Animals	F	196.0	430530	NE
Accipiter bicolor	Accipitridae	Birds	M	245.0	622236	NE
Accipiter cooperii	Accipitridae	Birds	M	349.0	636924	NE
Accipiter fasciatus	Accipitridae	Small Animals	M	510.0	620189	NE
Accipiter gentilis	Accipitridae	Birds	M	912.0	610353	NE
Accipiter haplochorus	Accipitridae	Small Animals	F	254.0	561511	NE
Accipiter henicogrammus	Accipitridae	Small Animals	F	-	556987	NE
Accipiter melanochlamys	Accipitridae	Birds	M	294.0	561484	NE
Accipiter melanoleucus	Accipitridae	Birds	M	695.0	291786	NE
Accipiter minullus	Accipitridae	Birds	M	75.7	490283	NE
Accipiter nisus	Accipitridae	Birds	F	325.0	344423	NE
Accipiter novaehollandiae griseogularis	Accipitridae	Small Animals	U	258.5	558270	NE
Accipiter poliogaster	Accipitridae	NO INFORMATION	F	-	622941	NE
Accipiter striatus velox	Accipitridae	Birds	M	103.0	553261	NE
Accipiter tachiro	Accipitridae	Birds	M	202.0	622998	NE

Accipiter virgatus confusus	Accipitridae	Birds	F	143.0	488909	NE
Aegypius monachus	Accipitridae	Carrion	U	9625.0	614152	PG
Aquila audax	Accipitridae	Large Vertebrates	M	3500.0	620192	PG
Aquila rapax	Accipitridae	Medium Vertebrates	F	2250.0	430406	PG
Aviceda subcristata	Accipitridae	Small animals	F	294.0	558306	NE
Busarellus nigricollis	Accipitridae	Fish	M	614.0	345773	NE
Butastur indicus	Accipitridae	Small Animals	U	397.0	223986	NE
Buteo albicaudatus	Accipitridae	Small Animals	F	884.0	632372	NE
Buteo albonotatus	Accipitridae	Small Animals	M	628.0	621080	NE
Buteo buteo	Accipitridae	Small Animals	F	969.0	554270	NE
Buteo jamaicensis	Accipitridae	Small Animals	U	1126.0	290346	NE
Buteo lagopus s.-johannis	Accipitridae	Small Animals	M	847.0	291309	NE
Buteo lineatus	Accipitridae	Small Animals	M	475.0	614338	NE
Buteo magnirostris	Accipitridae	Insects	M	269.0	288766	NE
Buteo nitidus	Accipitridae	Small Animals	M	-	623049	NE
Buteo platypterus	Accipitridae	Small Animals	F	490.0	613957	NE
Buteo polyosoma (poecilochorus)	Accipitridae	Small Animals	M	-	346398	NE
Buteo regalis	Accipitridae	Medium Vertebrates	M	1059.0	289973	NE
Buteo ridgwayi[l]	Accipitridae	Small Animals	F	-	226132	NE
Buteo rufinus	Accipitridae	Small Animals	U	1174.5	019535	NE
Buteo rufofuscus	Accipitridae	Small Animals	U	1164.3	431785	NE
Buteo solitarius	Accipitridae	Small Animals	F	606.0	622623	NE
Buteo swainsoni	Accipitridae	Small Animals	M	908.0	321986	NE

Buteogallus aequinoctialis	Accipitridae	Small Animals	F	715.0	621054	NE
Buteogallus anthracinus	Accipitridae	Small Animals	M	793.0	344053	NE
Buteogallus meridionalis	Accipitridae	Small Animals	U	808.0	560138	NE
Buteogallus urubitinga	Accipitridae	Small Animals	M	925.0	621696	NE
Caracara cheriway	Falconidae	Carrion	F	-	321805	NE
Caracara plancus	Falconidae	Carrion	U	893.5	630187	NE
Cathartes aura	Cathartidae	Carrion	U	1467.0	354339	NE
Cathartes burrovianus	Cathartidae	Carrion	M	953.0	622341	NE
Cathartes melambrotus	Cathartidae	Carrion	F	1200.0	621939	NE
Chondrohierax u. uncinatus	Accipitridae	Small Animals[3]	U	278.0	289784	NE
Circaetus cinereus	Accipitridae	Snakes	M	2048.0	430776	PG
Circaetus gallicus	Accipitridae	Snakes	F	1703.0	430827	NE
Circus aeruginosus	Accipitridae	Small Animals	M	492.0	344419	NE
Circus approximans	Accipitridae	Small Animals	U	705.0	492471	NE
Circus buffoni	Accipitridae	Small Animals	M	410.0	623127	NE
Circus cinereus	Accipitridae	Birds	U	420.0	321772	NE
Circus cyaneus hudsonius	Accipitridae	Small Animals	M	358.0	291684	NE
Circus maurus	Accipitridae	Birds	M	-	558448	NE
Coragyps atratus	Cathartidae	Carrion	M	2172.0	559659	PG
Daptrius ater	Falconidae	Carrion	F	342.0	226167	NE

Elanoides forficatus	Accipitridae	Insects	M	442.0	289686	NE
Elanus caeruleus	Accipitridae	Small Animals	F	350.0	558447	NE
Elanus leucurus	Accipitridae	Small Animals	U	300.0	19603	NE
Falco berigora	Falconidae	Small Animals	F	625.0	347646	NE
Falco biarmicus	Falconidae	Birds	U	593.0	620138	NE
Falco cherrug	Falconidae	Small Animals	F	1050.0	500262	NE
Falco columbarius	Falconidae	Birds	F	218.0	554550	NE
Falco eleonorae	Falconidae	Insects	M	390.0	488786	NE
Falco femoralis	Falconidae	Birds	F	407.0	622320	NE
Falco longipennis	Falconidae	Birds	M	213.0	347645	NE
Falco mexicanus	Falconidae	Small Animals	M	554.0	610758	NE
Falco moluccensis	Falconidae	Small Animals	F	-	558272	NE
Falco naumanni	Falconidae	Insects	F	164.0	603409	NE
Falco perigrinus anatum	Falconidae	Birds	M	611.0	291186	NE
Falco rufigularis	Falconidae	Birds	M	129.0	644063	NE
Falco rupicoloides	Falconidae	Small Animals	M	260.0	430626	NE
Falco rusticolis	Falconidae	Small Animals	F	1752.0	567722	NE
Falco sparverius dominicensis	Falconidae	Small Animals	M	111.0	555741	NE
Falco subbuteo	Falconidae	Insects	M	204.0	603410	NE
Falco tinnunculus	Falconidae	Small Animals	F	217.0	610374	NE
Falco verspertinus amurensis	Falconidae	Insects	U	165.5	289434	NE
Gampsonyx swainsonii	Accipitridae	Small Animals	F	92.5	623084	NE

Geranoaetus melanoleucus	Accipitridae	Medium Vertebrates	U	2252.0	318388	NE
Geranospiza caerulescens gracilis	Accipitridae	Small Animals	M	338.0	345774	NE
Gymnogyps californianus[l]	Cathartidae	Carrion	U	10104.0	492447	PG
Gypaetus barbatus	Accipitridae	Carrion [1]	F	5680.0	345684	PG
Gypohierax angolensis	Accipitridae	Generalist/Omnivore	F	1600.0	291078	NE
Gyps africanus	Accipitridae	Carrion	U	5300.0	19991	PG
Gyps coprotheres	Accipitridae	Carrion	U	8177.0	561314	PG
Gyps ruppelli	Accipitridae	Carrion	U	7400.0	430178	PG
Haliaeetus albicilla	Accipitridae	Fish	M	4014.0	292774	PG
Haliaeetus leucocephalus	Accipitridae	Generalist/Omnivore	U	7415.0	4882	PG
Haliaeetus vocifer	Accipitridae	Fish	M	2212.5	488146	NE
Haliastur indus	Accipitridae	Small Animals	F	450.0	556984	NE
Haliastur sphenurus	Accipitridae	Small Animals	M	800.0	610563	NE
Harpagus bidentatus	Accipitridae	Small Animals	F	239.0	612259	NE
Harpia harpjya	Accipitridae	Large Vertebrates	U	6200.0	432244	PG
Herpetotheres cachinnans	Falconidae	Snakes	F	715.0	289775	NE
Hieraeetus spilogaster	Accipitridae	Medium Vertebrates	M	1225.0	430796	NE
Ibycter americanus	Falconidae	Generalist/Omnivore	F	586.0	632410	NE
Icthyophaga humilis	Accipitridae	Fish	M	782.5	224807	NE
Icthyophaga icthyaetus	Accipitridae	Fish	U	2037.5	468555	NE

Ictinia misisippiensis	Accipitridae	Insects	M	245.0	610729	NE
Ictinia plumbea	Accipitridae	Insects	M	247.0	613355	NE
Kaupifalco monogrammicus	Accipitridae	Insects	M	311.5	322456	NE
Leptodon cayanensis	Accipitridae	Small Animals	M	484.0	613953	NE
Leucopternis albicollis	Accipitridae	Small Animals	M	600.0	613956	NE
Leucopternis melanops	Accipitridae	NO INFORMATION	F	307.0	432181	NE
Leucopternis princeps	Accipitridae	NO INFORMATION	M	1000.0	613281	NE
Leucopternis semiplumbea	Accipitridae	NO INFORMATION	F	325.0	613955	NE
Lophaetos occipitalis	Accipitridae	Small Animals	M	1140.0	291451	NE
Macheiramphus alcinus	Accipitridae	Birds [2]	U	650.0	559816	NE
Melierax canorus	Accipitridae	Small Animals	M	684.0	620139	NE
Melierax metabates mechawi	Accipitridae	Small Animals	M	598.0	430326	NE
Micrastur gilvicollis	Falconidae	Small Animals	M	204.0	637213	NE
Micrastur ruficollis	Falconidae	Small Animals	M	161.0	621387	NE
Micrastur semitorquatus	Falconidae	Small Animals	M	562.0	289773	NE
Microhierax caerculescens	Falconidae	Insects	F	40.0	499825	NE
Microhierax erythrogenys	Falconidae	Insects	F	43.5	613010	NE

Milvago chimachima cordatus	Falconidae	Carrion	U	332.5	343844	NE
Milvago chimango	Falconidae	Carrion	M	296.0	635870	NE
Milvus migrans	Accipitridae	Generalist/Omnivore	F	827.0	557810	NE
Necrosyrtes monachus	Accipitridae	Carrion	F	1813.0	291441	NE
Neophron percnopterus	Accipitridae	Carrion	U	2120.0	17835	PG
Pandion haliaetus	Pandionidae	Fish	F	1568.0	492597	NE
Parabuteo unicinctus	Accipitridae	Medium Vertebrates	M	690.0	630259	NE
Pernis ptilorhynchus gurneyi	Accipitridae	Insects	M	1066.0	343983	NE
Phalcoboenus australis	Falconidae	Carrion	F	1187.0	490890	NE
Phalcoboenus carunculatus	Falconidae	Generalist/Omnivore	F	-	614838	NE
Phalcoboenus megalopterus	Falconidae	Small Animals	U	795.0	500273	NE
Pithecophaga jefferyi[1]	Accipitridae	Large Vertebrates	M	4041.0	499879	PG
Polemaetus bellicosus	Accipitridae	Large Vertebrates	M	4230.0	430533	NE
Polihierax insignis	Falconidae	Small Animals	M	98.0	490664	NE
Polihierax semitorquatus	Falconidae	Small Animals	F	57.0	322394	NE
Polyboroides typus	Accipitridae	Small Animals	F	570.0	291787	NE
Rostrhamus sociabilis	Accipitridae	Small Animals[3]	M	378.0	631216	NE

Sagittarius serpentarius	Sagittaridae	Insects	F	3405.0	490786	PG
Sarcorhamphus papa	Cathartidae	Carrion	F	3400.0	320860	NE
Spilornis cheela	Accipitridae	Snakes	U	1072.0	19474	NE
Spizaetus ornatus	Accipitridae	Medium Vertebrates	M	1069.0	430495	NE
Spizaetus tyrannus	Accipitridae	Medium Vertebrates	M	1025.0	623090	NE
Spizastur melanoleucus	Accipitridae	Small Animals	U	850.0	321507	NE
Spiziapteryx circumcinctus	Falconidae	Small Animals	M	152.0	319445	NE
Stephanoaetus coronatus	Accipitridae	Large Vertebrates	F	3640.0	346655	NE
Terathopius ecuadatus	Accipitridae	Small Animals	F	2438.5	319919	PG
Torgos tracheliotus	Accipitridae	Carrion	M	7500.0	347597	PG
Trigonoceps occipitalis	Accipitridae	Carrion	U	5900.0	347358	PG
Urotuorchis macrourus batesi	Accipitridae	Small Animals	M	492.0	292398	NE
Vultur gryphus	Cathartidae	Carrion	M	12500.0	346633	PG

F, female; M, male; U, unknown; NE = NextEngine laser scanner; NMNH, Smithsonian Institution National Museum of Natural History; PG, photogrammetry

* Mass estimates taken from (*22*). Mass was taken for same sex birds wherever possible. Otherwise, species averages, opposite sex, or birds of unknown sex were used to estimate mass.

[1] *Gypaetus barbatus* is classified as a carrion eater, although its diet is almost exclusively comprised of bone

[2] *Macheirhamphus alcinus* is a specialist predator of bats, but is here classified as a bird eater

[3] *Chondrohierax uncinatus* and *Rostrhamus sociabilis* are both specialist predators of snails, but are classified here as small animal predators due to their small sample size.

[!] Critically Endangered [International Union for Conservation of Nature and Natural Resources (IUCN) Red List, 2015].

Table S3.

Euclidean NPMANOVA of PC scores from the beak block only. Bonferroni-corrected p-values showing differences between families.

	Accipitridae	Cathartidae	Falconidae
Accipitridae		0.0003	0.0003
Cathartidae	0.0003		0.0003
Falconidae	0.0003	0.0003	

Table S4.

Euclidean NPMANOVA of PC scores from the braincase block only. Bonferroni-corrected p-values showing differences between families.

	Accipitridae	Cathartidae	Falconidae
Accipitridae		0.0003	0.0003
Cathartidae	0.0003		0.0003
Falconidae	0.0003	0.0003	

Table S5.

Euclidean NPMANOVA of PC scores from the beak block only, with Bonferroni-corrected p-values showing differences between dietary groups. Bold values indicate significantly different pairings ($p < 0.05$).

	Small Animals	Medium Vertebrates	Large Vertebrates	Birds	Carrion	Insects	Fish	Snakes	Generalist/ Omnivore
Small Animals		1	0.0504	0.2088	**0.0036**	**0.0072**	1	1	**0.0036**
Medium Vertebrates	1		0.1188	0.234	**0.0036**	**0.0108**	1	1	**0.0252**
Large Vertebrates	0.0504	0.1188		**0.0072**	**0.0036**	**0.0252**	0.9504	1	0.1908
Birds	0.2088	0.234	**0.0072**		**0.0036**	0.1512	0.0936	0.1764	**0.0036**
Carrion	**0.0036**	**0.0036**	**0.0036**	**0.0036**		**0.0036**	0.1116	**0.0324**	1
Insects	**0.0072**	**0.0108**	**0.0252**	0.1512	**0.0036**		0.1404	0.1008	**0.0072**
Fish	1	1	0.9504	0.0936	0.1116	0.1404		1	1
Snakes	1	1	1	0.1764	**0.0324**	0.1008	1		0.8964
Generalist/ Omnivore	**0.0036**	**0.0252**	0.1908	**0.0036**	1	**0.0072**	1	0.8964	

Table S6.

Euclidean NPMANOVA of PC scores from the braincase block only, with Bonferroni-corrected p-values showing differences between dietary groups. Bold values indicate significantly different pairings ($p < 0.05$).

	Small Animals	Medium Vertebrates	Large Vertebrates	Birds	Carrion	Insects	Fish	Snakes	Generalist/ Omnivore
Small Animals		1	**0.0036**	**0.0072**	**0.0036**	0.8856	0.0684	**0.018**	**0.0036**
Medium Vertebrates	1		1	**0.0036**	0.0756	**0.018**	1	1	1
Large Vertebrates	**0.0036**	1		**0.0036**	0.4824	**0.0108**	0.1152	1	0.1836
Birds	**0.0072**	**0.0036**	**0.0036**		**0.0036**	0.3888	**0.0324**	**0.0072**	**0.0072**
Carrion	**0.0036**	0.0756	0.4824	**0.0036**		**0.0036**	1	0.1692	1
Insects	0.8856	**0.018**	**0.0108**	0.3888	**0.0036**		**0.0108**	**0.0144**	**0.0036**
Fish	0.0684	1	0.1152	**0.0324**	1	**0.0108**		0.108	1
Snakes	**0.018**	1	1	**0.0072**	0.1692	**0.0144**	0.108		0.8676
Generalist/ Omnivore	**0.0036**	1	0.1836	**0.0072**	1	**0.0036**	1	0.8676	